CLEO CONF 97-22a
EPS97-333

Study of Charmless Hadronic Decays of B Mesons With Final States Including η or η' Mesons

CLEO Collaboration

(August 14, 1997)

Abstract

Using all available data collected at CESR with the CLEO II detector, we have studied exclusive charmless hadronic decays of B mesons with η or η' mesons in the final state. A signal significantly larger than theoretical predictions is observed in the $B^+ \to \eta' K^+$ decay channel, with a branching fraction of $\mathcal{B}(B^+ \to \eta' K^+) = (7.1^{+2.5}_{-2.1} \pm 0.9) \times 10^{-5}$ and a statistical significance of 5.8σ. We also have confirming evidence in the neutral companion to this mode, $B^0 \to \eta' K^0$, with a branching fraction of $(5.3^{+2.8}_{-2.2} \pm 1.2) \times 10^{-5}$ and a statistical significance of 4.3σ. Finally, we set limits for other related modes that have interesting theoretical implications.

S. Anderson,[1] Y. Kubota,[1] S. J. Lee,[1] J. J. O'Neill,[1] S. Patton,[1] R. Poling,[1] T. Riehle,[1] V. Savinov,[1] A. Smith,[1] M. S. Alam,[2] S. B. Athar,[2] Z. Ling,[2] A. H. Mahmood,[2] H. Severini,[2] S. Timm,[2] F. Wappler,[2] A. Anastassov,[3] J. E. Duboscq,[3] D. Fujino,[3,*] K. K. Gan,[3] T. Hart,[3] K. Honscheid,[3] H. Kagan,[3] R. Kass,[3] J. Lee,[3] M. B. Spencer,[3] M. Sung,[3] A. Undrus,[3,†] R. Wanke,[3] A. Wolf,[3] M. M. Zoeller,[3] B. Nemati,[4] S. J. Richichi,[4] W. R. Ross,[4] P. Skubic,[4] M. Bishai,[5] J. Fast,[5] J. W. Hinson,[5] N. Menon,[5] D. H. Miller,[5] E. I. Shibata,[5] I. P. J. Shipsey,[5] M. Yurko,[5] S. Glenn,[6] S. D. Johnson,[6] Y. Kwon,[6,‡] S. Roberts,[6] E. H. Thorndike,[6] C. P. Jessop,[7] K. Lingel,[7] H. Marsiske,[7] M. L. Perl,[7] D. Ugolini,[7] R. Wang,[7] X. Zhou,[7] T. E. Coan,[8] V. Fadeyev,[8] I. Korolkov,[8] Y. Maravin,[8] I. Narsky,[8] V. Shelkov,[8] J. Staeck,[8] R. Stroynowski,[8] I. Volobouev,[8] J. Ye,[8] M. Artuso,[9] A. Efimov,[9] M. Goldberg,[9] D. He,[9] S. Kopp,[9] G. C. Moneti,[9] R. Mountain,[9] S. Schuh,[9] T. Skwarnicki,[9] S. Stone,[9] G. Viehhauser,[9] X. Xing,[9] J. Bartelt,[10] S. E. Csorna,[10] V. Jain,[10,§] K. W. McLean,[10] S. Marka,[10] R. Godang,[11] K. Kinoshita,[11] I. C. Lai,[11] P. Pomianowski,[11] S. Schrenk,[11] G. Bonvicini,[12] D. Cinabro,[12] R. Greene,[12] L. P. Perera,[12] G. J. Zhou,[12] B. Barish,[13] M. Chadha,[13] S. Chan,[13] G. Eigen,[13] J. S. Miller,[13] C. O'Grady,[13] M. Schmidtler,[13] J. Urheim,[13] A. J. Weinstein,[13] F. Würthwein,[13] D. W. Bliss,[14] G. Masek,[14] H. P. Paar,[14] S. Prell,[14] V. Sharma,[14] D. M. Asner,[15] J. Gronberg,[15] T. S. Hill,[15] D. J. Lange,[15] S. Menary,[15] R. J. Morrison,[15] H. N. Nelson,[15] T. K. Nelson,[15] C. Qiao,[15] J. D. Richman,[15] D. Roberts,[15] A. Ryd,[15] M. S. Witherell,[15] R. Balest,[16] B. H. Behrens,[16] W. T. Ford,[16] H. Park,[16] J. Roy,[16] J. G. Smith,[16] J. P. Alexander,[17] C. Bebek,[17] B. E. Berger,[17] K. Berkelman,[17] K. Bloom,[17] D. G. Cassel,[17] H. A. Cho,[17] D. S. Crowcroft,[17] M. Dickson,[17] P. S. Drell,[17] K. M. Ecklund,[17] R. Ehrlich,[17] A. D. Foland,[17] P. Gaidarev,[17] L. Gibbons,[17] B. Gittelman,[17] S. W. Gray,[17] D. L. Hartill,[17] B. K. Heltsley,[17] P. I. Hopman,[17] J. Kandaswamy,[17] P. C. Kim,[17] D. L. Kreinick,[17] T. Lee,[17] Y. Liu,[17] G. S. Ludwig,[17] N. B. Mistry,[17] C. R. Ng,[17] E. Nordberg,[17] M. Ogg,[17,**] J. R. Patterson,[17] D. Peterson,[17] D. Riley,[17] A. Soffer,[17] B. Valant-Spaight,[17] C. Ward,[17] M. Athanas,[18] P. Avery,[18] C. D. Jones,[18] M. Lohner,[18] C. Prescott,[18] J. Yelton,[18] J. Zheng,[18] G. Brandenburg,[19] R. A. Briere,[19] A. Ershov,[19] Y. S. Gao,[19] D. Y.-J. Kim,[19] R. Wilson,[19] H. Yamamoto,[19] T. E. Browder,[20] Y. Li,[20] J. L. Rodriguez,[20] T. Bergfeld,[21] B. I. Eisenstein,[21] J. Ernst,[21] G. E. Gladding,[21] G. D. Gollin,[21] R. M. Hans,[21] E. Johnson,[21] I. Karliner,[21] M. A. Marsh,[21] M. Palmer,[21] M. Selen,[21] J. J. Thaler,[21] K. W. Edwards,[22] A. Bellerive,[23] R. Janicek,[23] D. B. MacFarlane,[23] P. M. Patel,[23] A. J. Sadoff,[24] R. Ammar,[25] P. Baringer,[25] A. Bean,[25] D. Besson,[25] D. Coppage,[25] C. Darling,[25] R. Davis,[25] N. Hancock,[25] S. Kotov,[25] I. Kravchenko,[25] and N. Kwak[25]

---

[*]Permanent address: Lawrence Livermore National Laboratory, Livermore, CA 94551.

[†]Permanent address: BINP, RU-630090 Novosibirsk, Russia.

[‡]Permanent address: Yonsei University, Seoul 120-749, Korea.

[§]Permanent address: Brookhaven National Laboratory, Upton, NY 11973.

[**]Permanent address: University of Texas, Austin TX 78712

[1]University of Minnesota, Minneapolis, Minnesota 55455
[2]State University of New York at Albany, Albany, New York 12222
[3]Ohio State University, Columbus, Ohio 43210
[4]University of Oklahoma, Norman, Oklahoma 73019
[5]Purdue University, West Lafayette, Indiana 47907
[6]University of Rochester, Rochester, New York 14627
[7]Stanford Linear Accelerator Center, Stanford University, Stanford, California 94309
[8]Southern Methodist University, Dallas, Texas 75275
[9]Syracuse University, Syracuse, New York 13244
[10]Vanderbilt University, Nashville, Tennessee 37235
[11]Virginia Polytechnic Institute and State University, Blacksburg, Virginia 24061
[12]Wayne State University, Detroit, Michigan 48202
[13]California Institute of Technology, Pasadena, California 91125
[14]University of California, San Diego, La Jolla, California 92093
[15]University of California, Santa Barbara, California 93106
[16]University of Colorado, Boulder, Colorado 80309-0390
[17]Cornell University, Ithaca, New York 14853
[18]University of Florida, Gainesville, Florida 32611
[19]Harvard University, Cambridge, Massachusetts 02138
[20]University of Hawaii at Manoa, Honolulu, Hawaii 96822
[21]University of Illinois, Champaign-Urbana, Illinois 61801
[22]Carleton University, Ottawa, Ontario, Canada K1S 5B6
and the Institute of Particle Physics, Canada
[23]McGill University, Montréal, Québec, Canada H3A 2T8
and the Institute of Particle Physics, Canada
[24]Ithaca College, Ithaca, New York 14850
[25]University of Kansas, Lawrence, Kansas 66045

I. INTRODUCTION

There has been much progress in measurement of charmless hadronic B decays by the CLEO II collaboration during the past year. There is a great deal of interest in these modes since they are expected to proceed predominantly through $b \to u$ spectator diagrams, which are suppressed by the small CKM element V_{ub}, or through "penguin" loop diagrams. We reported in March [1] clear evidence for the decay $B^0 \to K^+\pi^{-1}$. The observation of the modes $B^+ \to \omega K^+$ and $B^+ \to \omega\pi^+$ with surprisingly large branching fractions was reported last summer [2] and a more refined analysis was presented in March at Hawaii [1]. Further results for this analysis are reported in another contribution to this conference [3].

Perhaps the most surprising of all of the recent measurements was the observation of the decay $B^+ \to \eta' K^+$, reported in January, [4] with results for a variety of related modes presented in March [1]. The branching fraction for this decay was found to be $(7.8^{+2.7}_{-2.2} \pm 1.0) \times 10^{-5}$. While this decay was expected to be somewhat larger than other charmless hadronic B decays, the measured branching fraction is about two standard deviations larger than the largest previous theoretical predictions of 1-4$\times 10^{-5}$ [5–7]. Such predictions use a combination of effective Hamiltonian methods for the perturbative, short-distance part of the calculation and factorization assumptions and empirical form factors for the non-perturbative, long-distance piece. Clear descriptions of such techniques can be found in many papers [8].

The fact that other related modes such as $B^+ \to \eta K^+$ are found to be greatly suppressed [1] was predicted by Lipkin in 1991 [9]. The suppression is the result of constructive interference in the case of η' and destructive interference in the case of η for the two penguin diagrams shown in Fig. 1. We also reported in March [1] and in another contribution to this conference [10], a surprisingly large rate for the inclusive process $B \to \eta' X$ for η' mesons with momenta above 2 GeV/c.

There have been many recent theoretical attempts to explain these unexpected experimental results. Berkelman [11] and others in CLEO have suggested that there may be a substantial component from the spectator $b \to c\bar{c}s$ decay as a result of a $c\bar{c}$ component of the η' (i.e. η_c-η' mixing). This idea has recently been addressed by Yuan and Chao [12] and Ali and Greub [13]. Though they claim to set stringent limits on this process using the decays $\psi \to \eta_c\gamma$ and $\psi \to \eta'\gamma$, they appear to have omitted the overlap integral, which is important for the latter decay since the η' is highly relativistic. Cheng and Tseng [14] note that η_c-η' mixing at a level eight times as large as that used in Refs. [12,13] would account for the experimental result. Two recent models involve an intrinsic charm component of the η'. A model by Zhitnitsky *et al.* [15] has a color singlet $c\bar{c}$ component while Yuan and Chao [12] have a model with a color-octet component. Dunietz *et al.* [16], also envisioned a color-octet contribution to this process though their paper lacks quantitative predictions. Were the intrinsic charm component the dominant contribution to this process, both of these models would predict the branching fraction for $B^+ \to \eta' K^{*+}$ to be twice that of $B^+ \to \eta' K^+$.

Recently two papers have suggested that there is no problem accounting for a large rate

---

[1]Charge conjugate modes are implied throughout the paper.

for $B^+ \to \eta' K^+$. Datta, He and Pakvasa [17] suggest that the predicted rate is much larger if the form factors from Ref. [6] are used. Kagan and Petrov [18] also find a somewhat larger value by varying the model inputs. However their use of a small strange quark mass (100 MeV rather than the 200 MeV which is normally used) may be in conflict with a recent measurement, $m_s(m_\tau) = 212^{+30}_{-35}$ MeV [19].

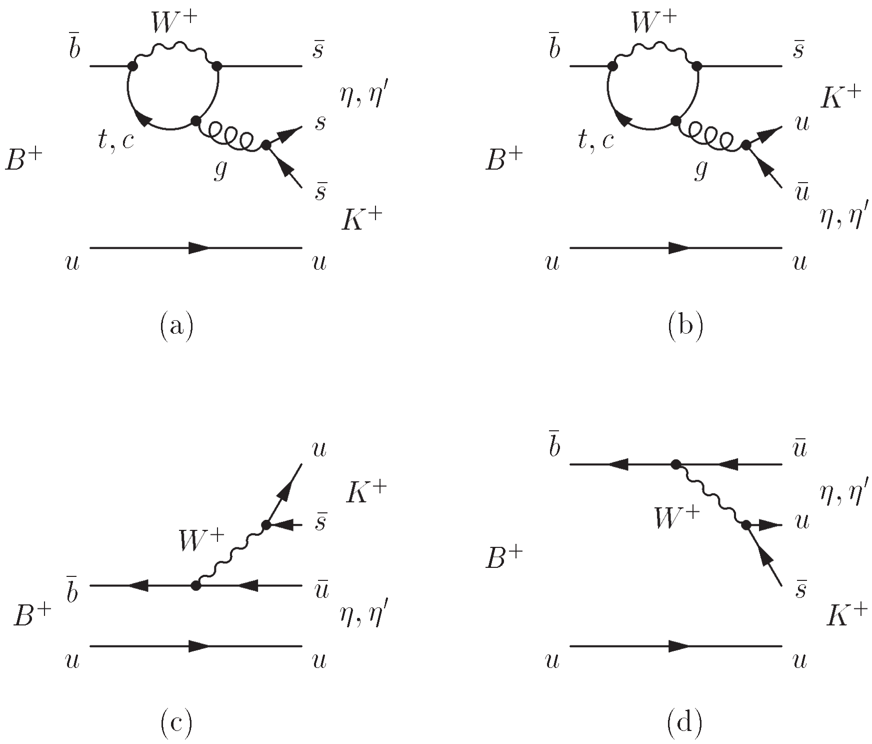

FIG. 1. Feynman diagrams contributing to the decay modes of interest in this paper. Modes with a K^*, K^0 or ρ involve slight modifications with a d spectator quark or a d quark replacing an s quark in these diagrams.

In this paper we update the previous analysis of $B^+ \to \eta' K^+$ with a somewhat improved efficiency and also provide limits for other decays involving η and η'.

II. DATA SAMPLE AND INITIAL EVENT SELECTION

All results presented here are based on data collected with the CLEO II detector [20] at the Cornell Electron Storage Ring (CESR). The data sample corresponds to an integrated luminosity of 3.11 fb^{-1} taken on the $\Upsilon(4S)$ resonance and 1.61 fb^{-1} taken slightly below. The on-resonance data sample contains 3.3×10^6 $B\overline{B}$ pairs. The detector elements most important for the analyses presented here are the tracking system, which is used to measure the momentum and energy loss rate (dE/dx) of charged particles, and the CsI crystal calorimeter, which is used to measure the energy of photons. We reconstruct particles in the final state with the following decay channels : $\eta' \to \pi^+\pi^-\eta$, $\eta' \to \rho^0\gamma$, $K^{*0} \to K^+\pi^-$, $K^{*+} \to K^+\pi^0$, K^0 via $K_S \to \pi^+\pi^-$, $\rho^0 \to \pi^+\pi^-$, $\pi^0 \to \gamma\gamma$ and $\eta \to \gamma\gamma$. In some cases, we also use $\eta \to \pi^+\pi^-\pi^0$.

Two analysis techniques are used to extract the results: An event-counting method, in which events that satisfy a series of cuts are taken as signal for the decay mode investigated, and a maximum likelihood method. A number of preliminary cuts are applied for both these techniques. The total number of charged tracks in each event is required to be at least two greater than the number from the candidate B meson. Reconstruction and quality cuts for charged tracks and showers are as described in Ref. [21]. However, the cut positions for charged track quality cuts are loosened compared to earlier analyses. This accounts for the increased efficiency for the analysis of some decay modes already reported. The measured dE/dx of charged pions and kaons is required to be within 3σ of the expected value. Electrons are rejected based on dE/dx and the ratio of the measured track momentum and the associated shower energy in the calorimeter. Muons are rejected by requiring that the track penetrate less than five interaction lengths of material. Pairs of charged tracks used to reconstruct K_S's are required to have a common vertex displaced from the primary interaction point by at least 3 mm.

Pairs of showers used to reconstruct π^0's are required to have an invariant mass within two standard deviations of the nominal π^0 mass. The π^0 or η momentum are obtained with a kinematic fit of the photon momenta with the particle mass constrained to its nominal value. To reduce combinatoric background, the momenta of π^0's, η's and charged particles used to form a candidate B meson are required to be greater than 175 MeV/c. For maximum likelihood analyses, the minimum momentum for charged particles is 100 MeV/c.

III. EVENT-COUNTING ANALYSES

A. FINAL EVENT SELECTION

The final cuts for the event-counting analyses are designed to reduce the large background from continuum $q\bar{q}$ production while maintaining high efficiency for signal. The cut positions are chosen to optimize the expected branching ratio upper limit. The largest background rejection is obtained with event shape cuts. These rely on the fact that at the $\Upsilon(4S)$ B mesons are produced almost at rest. The decay products of the $B\bar{B}$ pair tend to be spherically distributed, while particles from $q\bar{q}$ production have a more jet-like distribution. Two event shape cuts are used in these analyses. First, the angle θ_T between the thrust axis of the charged particles and photons forming the candidate B and the thrust axis of the remainder of the event, is required to satisfy $|\cos\theta_T| < 0.9$; for this variable, continuum background is strongly peaked near 1.0 and signal is approximately flat. Second, a Fisher discriminant ($\mathcal{F}$) is formed with 11 variables: the scalar momentum sum of charged particles and photons in nine cones of increasing polar angle around the thrust axis of the candidate, the angle between the thrust axis of the candidate and the beam axis, and the angle between the candidate B direction and the beam axis. This discriminant is described in detail in Ref. [21]. For this variable, signal peaks around 0.4 and background around 0.7. In each case, the low side of the distribution has a σ of ~ 0.13 and the high side ~ 0.17. The cut position varies depending on the decay mode investigated. Table II lists the value of the cut for each decay mode.

Cuts on the reconstructed invariant mass of particles are listed in Table I. For decay modes with a K^* (ρ) in the final state, we cut on the angle θ_h between the direction of the parent B meson and the direction of the charged decay products of the K^* (ρ), both calculated in the rest frame of the K^* (ρ). We expect signal to have a distribution proportional to $\cos^2\theta_h$, while background will be nearly flat. We require $|\cos\theta_h| > 0.5$.

TABLE I. Invariant mass cuts for event-counting analyses.

Particle	Decay mode	Cut
η'	$\eta\pi^+\pi^-$	$\lvert M_{\eta\pi^+\pi^-} - 957.5\rvert < 9$ MeV/c^2
η	$\gamma\gamma$	$\lvert M_{\gamma\gamma} - 545\rvert < 30$ MeV/c^2
η	$\pi^+\pi^-\pi^0$	$\lvert M_{\pi^+\pi^-\pi^0} - 545\rvert < 10$ MeV/c^2
K^{*0}	$K^+\pi^-$	$\lvert M_{K^+\pi^-} - 896\rvert < 75$ MeV/c^2
K^{*+}	$K^+\pi^0$	$\lvert M_{K^+\pi^0} - 896\rvert < 75$ MeV/c^2
ρ^0	$\pi^+\pi^-$	$\lvert M_{\pi^+\pi^-} - 768.5\rvert < 150$ MeV/c^2

Final candidate selection is based on the energy and mass of the candidate B. For the energy, we define the quantity $\Delta E = E_1 + E_2 - E_b$, where E_1 and E_2 are the energy of the two daughter particles of the B and E_b is the beam energy. ΔE should peak at 0 for B mesons, and have a linearly falling distribution for continuum background. The beam-constrained mass of the candidate is defined as $M_B = \sqrt{E_b^2 - p_B^2}$, where p_B is the measured momentum of the candidate. Using the beam energy instead of the measured energy of the B candidate improves the mass resolution by about an order of magnitude, with the resolution dominated by the energy spread of the beam. The measured resolutions for signal Monte Carlo are approximately 30 MeV and 2.7 MeV/c^2 for ΔE and M_B, respectively. Candidates are selected in the region $|M_B - 5280| < 6$ MeV/c^2 and $|\Delta E| < 60$ MeV.

B. BACKGROUND ESTIMATE AND RESULTS

The expected number of background events after all cuts is based on an estimate of the ratio $\mathcal{A}$ defined as the number of events in the ΔE—M_B signal region divided by the number of events in a "grand sideband" region ($|\Delta E| < 0.2$ GeV and $5.2 < M_B < 5.27$ GeV/c^2). The ratio is determined from a sample of Monte Carlo simulated continuum events about twice as large as the on-resonance data sample. To further increase the statistical accuracy of the measurement, cuts not affecting the ratio are released. Values of $\mathcal{A}$ vary slightly depending on the decay mode, and are in the range 0.03–0.04. The background estimate for each decay mode studied is obtained by multiplying the measured ratio $\mathcal{A}$ by the number of events observed in the grand sideband for the on-resonance data sample after all other cuts are applied.

Background from $b \to c$ decays is studied with a Monte Carlo generated sample approximately four times as large as the data sample. The contribution from this source is found to be negligible.

Table II gives the results for each mode. In this table $\eta_{3\pi}$, $\eta_{\gamma\gamma}$ and η_{comb} refer to $\eta \to \pi^+\pi^-\pi^0$, $\eta \to \gamma\gamma$ and the sum of the two modes, respectively. Also, h^+ refers to either a charged pion or a charged kaon. Included in the table are the number of observed events (N_S), the estimated number of background events (N_B) with its combined statistical and systematic uncertainty, the efficiency for signal Monte Carlo events (ϵ), which does not include the branching ratios of particles in the final state, the total efficiency (ϵ_{tot}) with its associated systematic error, and the branching ratio ($\mathcal{B}$) upper limit at the 90% confidence level. The upper limits on the number of signal events are determined with the standard calculation for Poisson upper limits in the presence of background [22]. In the calculation of the upper limit, we reduced both the background estimate and the efficiency by one standard deviation of their error to take the systematic uncertainty into account.

TABLE II. Final results for event-counting analyses. Branching fraction upper limits are at the 90% confidence level.

Mode	$\mathcal{F}$ cut	N_S	N_B	$\epsilon(\%)$	$\epsilon_{tot}(\%)$	$\mathcal{B}(\times 10^{-5})$
$\eta_{3\pi}h^+$	< 0.50	0	0.7 ± 0.2	12	2.8 ± 0.4	< 2.8
$\eta_{\gamma\gamma}h^+$	< 0.45	0	1.5 ± 0.2	16	6.4 ± 0.6	< 1.2
$\eta_{comb}h^+$		0	2.2 ± 0.4	28	9.2 ± 1.0	< 0.8
$\eta_{3\pi}K^{*0}$	< 0.55	0	0.5 ± 0.2	6.0	0.9 ± 0.1	< 8.3
$\eta_{\gamma\gamma}K^{*0}$	< 0.50	1	0.8 ± 0.2	9.2	2.4 ± 0.2	< 4.1
$\eta_{comb}K^{*0}$		1	1.3 ± 0.3	15	3.3 ± 0.3	< 3.3
$\eta_{3\pi}K^{*+}$	< 0.55	0	0.5 ± 0.2	4.6	0.35 ± 0.06	< 24
$\eta_{3\pi}\rho^0$	< 0.55	1	0.8 ± 0.2	6.0	1.4 ± 0.2	< 8.4
$\eta' K^{*0}$	< 0.65	0	0.3 ± 0.1	7.1	0.8 ± 0.1	< 9.9
$\eta' K^{*+}$	< 0.70	0	0.3 ± 0.1	4.8	0.28 ± 0.04	< 29

IV. MAXIMUM LIKELIHOOD ANALYSES

A. METHOD

Unbinned maximum likelihood fits are performed to obtain signal yields for the decay modes $B^+ \to \eta' K^+$, $B^+ \to \eta' \pi^+$, $B^0 \to \eta' K^0$, $B^0 \to \eta' \pi^0$, $B^0 \to \eta K^0$, and $B^0 \to \eta \pi^0$. The quantities M_B, ΔE, and $\mathcal{F}$ are used as input information to the fit in all cases. We also use as appropriate $M_{\eta'}$, M_η, M_ρ, and M_{K_S}, the reconstructed invariant masses of η', η, ρ, and K_S particles. For the modes $B^+ \to \eta' K^+$ and $B^+ \to \eta' \pi^+$ we perform a simultaneous fit. In this case, to resolve the ambiguity in the identity of the high-momentum charged track, we use the fact that ΔE is computed assuming that the charged track is a kaon. If the track is a pion, the whole distribution is shifted by +44 MeV. For these modes we also include the dE/dx information as input to the fit. The quantity used is

$$S_K = \frac{(dE/dx)_{\text{measured}} - (dE/dx)_{\text{K hypothesis}}}{\sigma}, \tag{1}$$

where σ is the expected resolution. As for ΔE, this variable will have a distribution centered on zero for kaons and will be shifted for pions.

For N input events, the likelihood is defined as

$$\mathcal{L} = e^{-(N_S+N_B)} \prod_{i=1}^{N} \{N_S \mathcal{P}_S(f_1, ..., f_m; x_i) + N_B \mathcal{P}_B(f_1, ..., f_m; x_i)\}, \quad (2)$$

where $\mathcal{P}_S$ and $\mathcal{P}_B$ are the probabilities for event i with input quantities x_i and parameters f_j to be signal and continuum background, respectively. N_S and N_B, the free parameters of the fit, are the number of signal and continuum background events in the fitted data sample, respectively. The exponential factor preceding the product ensures that $N_S + N_B$ is equal to the total number of input events. For the simultaneous fit of $B^+ \to \eta' K^+$ and $B^+ \to \eta' \pi^+$, the likelihood is defined as

$$\mathcal{L} = e^{-(N_S^\pi + N_S^K + N_B)} \prod_{i=1}^{N} \{N_S^\pi \mathcal{P}_S^\pi + N_S^K \mathcal{P}_S^K + N_B [f_B^K \mathcal{P}_B^K + (1 - f_B^K) \mathcal{P}_B^\pi]\}, \quad (3)$$

where the π and K superscripts refer to the hypothesis made for the ambiguous charged track and f_B^K is the fraction of continuum background events for which the ambiguous charged track is a kaon. The latter is also a free parameter of the maximum likelihood fit.

The probability distribution functions are determined by separate fits to signal Monte Carlo and grand sideband data for $\mathcal{P}_S$ and $\mathcal{P}_B$, respectively. For M_B and $M_{\eta'}$ signal we use Gaussian functions; for ΔE, M_η, M_ρ, and M_{K_S} signal we use double Gaussians; and for $\mathcal{F}$ and S_K signal and background we use bifurcated Gaussians. For $M_{\eta'}$, M_η, M_ρ, and M_{K_S} background we use the sum of a first-degree polynomial and the signal shape to describe the pure combinatoric background and the component of real particles in the background. Finally, for ΔE the background is described by a first-degree polynomial and for M_B we use the empirical shape

$$f(M_B) \propto M_B \sqrt{1 - x^2} \exp\left(-\xi(1 - x^2)\right), \quad (4)$$

where $x \equiv M_B/E_b$ and ξ is a parameter to be fit.

Before performing the likelihood fit, a number of preliminary cuts are applied. We require all events to satisfy $|\cos\theta_T| < 0.9$. We also require $|\Delta E| < 0.2$ GeV, $5.2 < M_B < 5.3$ GeV/c^2, and as required $0.5 < M_\eta < 0.6$ GeV/c^2, $0.47 < M_{K_S} < 0.53$ GeV/c^2, and $0.93 < M_{\eta'} < 0.99$ GeV/c^2.

B. RESULTS

Table III gives the results of the maximum likelihood analyses. Shown in the table are the efficiency for signal Monte Carlo events, the total efficiency (including relevant branching fractions) and its associated systematic error, the signal yields, the statistical significance of the yield in number of standard deviations, and the calculated branching ratio. It should be emphasized that the significance does not include systematic effects. The 90% confidence level upper limit on the yield is determined by finding the point at which the integral of the likelihood curve is at 90% of its total. To take systematic errors on the fit yield into account, we increase the calculated upper limit by 15%. We also reduce the efficiency by one standard deviation in the calculation of the upper limit. The first error on the quoted branching fractions is statistical and the second systematic. The systematic error includes a contribution from the efficiency and a contribution from changes in fit yield that depend on variations in the parameters of the probability distribution functions. For $B^+ \to \eta' \pi^+$ and $B^0 \to \eta K^0$ we report the results as upper limits since the observed non-zero yields are not statistically significant.

Fig. 2 shows the maximum likelihood fit contours in 1σ increments for $B^+ \to \eta' K^+$ and $B^+ \to \eta' \pi^+$. The statistical significance of the $B^+ \to \eta' K^+$ signal is 5.8σ. Figs. 3 and 4 show projections of M_B and ΔE for this mode . Note that for the data histogram, cuts are applied to the likelihood fit input quantities other than the one plotted. The likelihood fit curves overlayed on the data are not a fit to the data shown but rather show the overall fit, scaled to take the effect of the additional cuts into account. Fig. 5 shows the value of $-2 \ln \mathcal{L}$ as a function of the branching fraction for the sum of the two $B^0 \to \eta' K^0$ analyses. The minimum of the curve corresponds to the combined branching fraction quoted in Table III. Within its large uncertainty, this result is in agreement with the measured $B^+ \to \eta' K^+$ signal. Figs. 6 and 7 show the projections of M_B and ΔE for $B^0 \to \eta' K^0$. Again, cuts have been applied to quantities other than the one plotted before making the projection.

TABLE III. Results from maximum likelihood analyses. Branching fraction upper limits are at the 90% confidence level. The significance is given in standard deviation units.

Mode	$\epsilon(\%)$	$\epsilon_{tot}(\%)$	N_{sig}	Signif.	$\mathcal{B}(\times 10^{-5})$
$\eta_{\gamma\gamma} K^0$	32	4.3 ± 0.4	3.6	1.8	< 7.5
$\eta_{\gamma\gamma} \pi^0$	32	12 ± 1	0.0	0.0	< 1.1
$\eta' K^+$	30	5.1 ± 0.6	12	5.8	$7.1^{+2.5}_{-2.1} \pm 0.9$
$\eta' K^0$	-	-	-	4.3	$5.3^{+2.8}_{-2.2} \pm 1.2$
$(\eta' \to \pi^+\pi^-\eta)$	23	1.4 ± 0.2	1.6	2.9	$3.5^{+3.7}_{-2.2} \pm 0.8$
$(\eta' \to \rho^0\gamma)$	27	2.8 ± 0.4	6.4	3.2	$6.9^{+4.1}_{-3.1} \pm 1.4$
$\eta' \pi^+$	28	4.8 ± 0.6	1.3	1.5	< 4.5
$\eta' \pi^0$	25	4.3 ± 0.5	0.0	0.0	< 2.2

V. CONCLUSION

We have searched for a variety of B-meson decays involving η or η' mesons. An unbinned maximum-likelihood analysis finds a 5.8σ excess for the mode $B^+ \to \eta' K^+$, with a branching fraction $\mathcal{B}(B^+ \to \eta' K^+) = (7.1^{+2.5}_{-2.1} \pm 0.9) \times 10^{-5}$. With the same analysis technique, we find confirming evidence for the companion neutral decay $B^0 \to \eta' K^0$, with a branching fraction of $\mathcal{B}(B^0 \to \eta' K^0) = (5.3^{+2.8}_{-2.2} \pm 1.2) \times 10^{-5}$ and a statistical significance of 4.3σ. We also set limits for other modes, demonstrating that the branching fraction for the decay $B^+ \to \eta K^+$ is much smaller than $B^+ \to \eta' K^+$, as expected, and that $B^+ \to \eta' K^{*+}$ is at most comparable to $B^+ \to \eta' K^+$, not twice as large, as would be expected in the intrinsic charm models.

VI. ACKNOWLEDGMENTS

We gratefully acknowledge the effort of the CESR staff in providing us with excellent luminosity and running conditions. We thank A. Ali, T. DeGrand, P. Lepage, H. Lipkin, A.

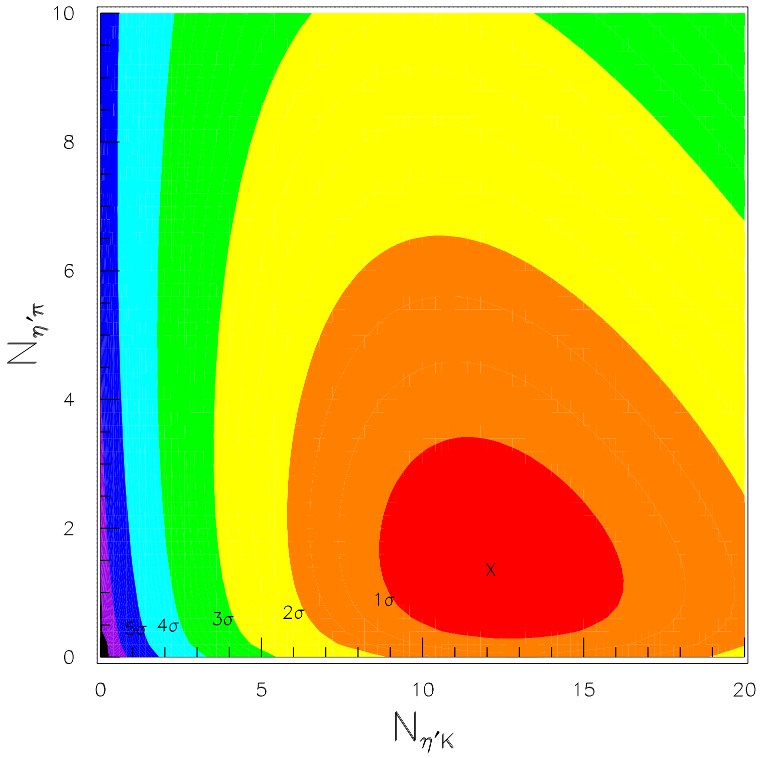

FIG. 2. Maximum likelihood fit contours in 1σ increments (statistical error only) for $B^+ \to \eta' K^+$ and $B^+ \to \eta' \pi^+$.

Kagan, and A. Soni for many useful discussions. J.P.A., J.R.P., and I.P.J.S. thank the NYI program of the NSF, M.S. thanks the PFF program of the NSF, G.E. thanks the Heisenberg Foundation, K.K.G., M.S., H.N.N., T.S., and H.Y. thank the OJI program of DOE, J.R.P., K.H., M.S. and V.S. thank the A.P. Sloan Foundation, R.W. thanks the Alexander von Humboldt Stiftung, and M.S. thanks Research Corporation for support. This work was supported by the National Science Foundation, the U.S. Department of Energy, and the Natural Sciences and Engineering Research Council of Canada.

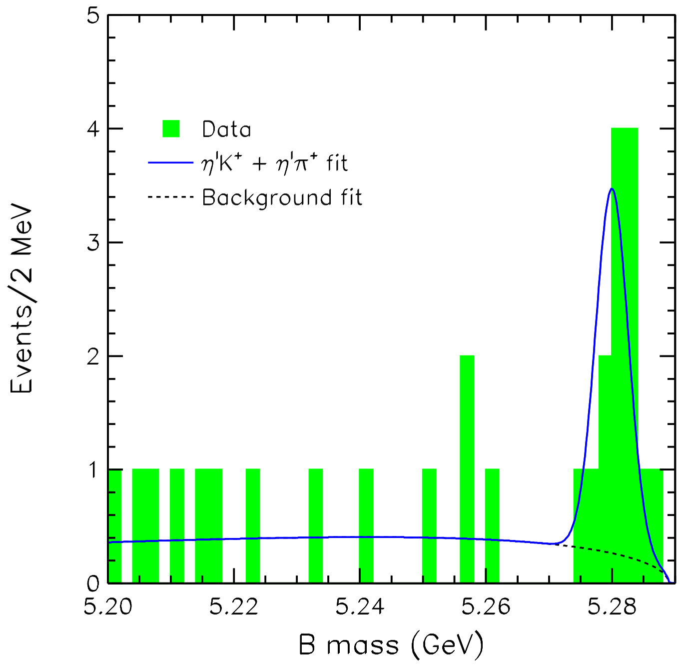

FIG. 3. Projection of M_B for $B^+ \to \eta' K^+$ and $B^+ \to \eta' \pi^+$. Cuts on all other input quantities to the fit have been applied before making the projection. The histogram shows the data, the smooth curve the scaled likelihood fit and the dashed curve shows the background component of the fit.

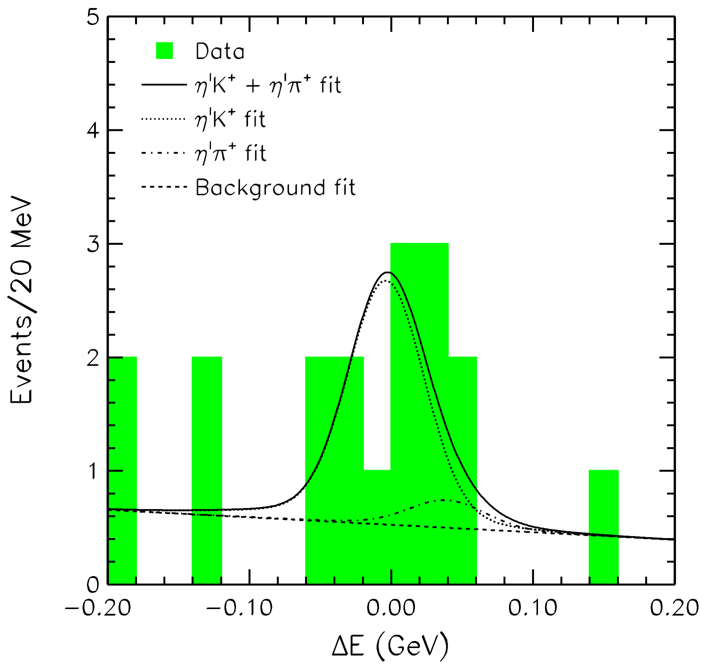

FIG. 4. Projection of ΔE for $B^+ \to \eta' K^+$ and $B^+ \to \eta' \pi^+$. Histograms and curves are as above, with separate K and π contributions of the fit indicated.

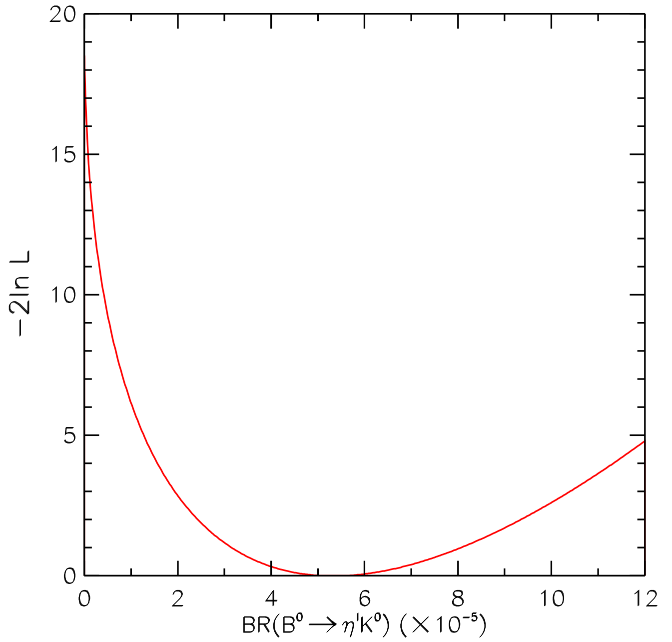

FIG. 5. $-2\ln\mathcal{L}$ as a function of the branching fraction for $B^0 \to \eta' K^0$.

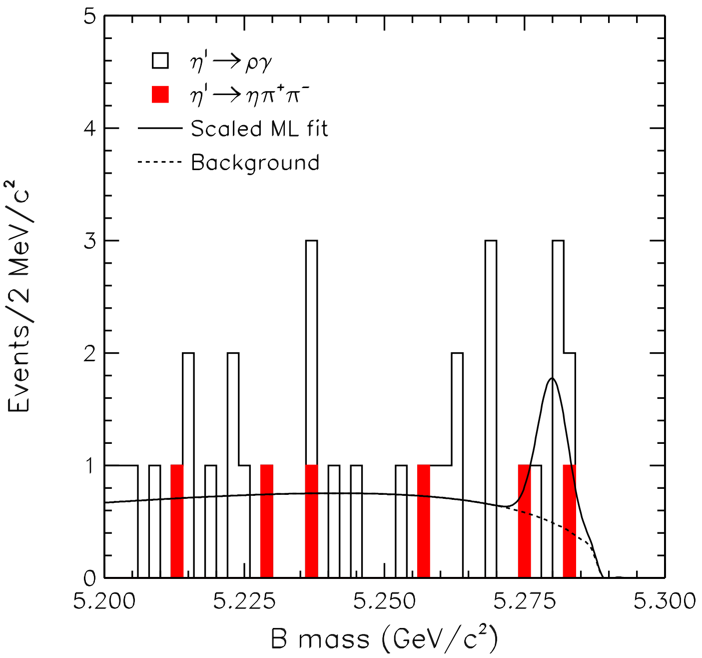

FIG. 6. Projection of M_B for $B^0 \to \eta' K^0$.

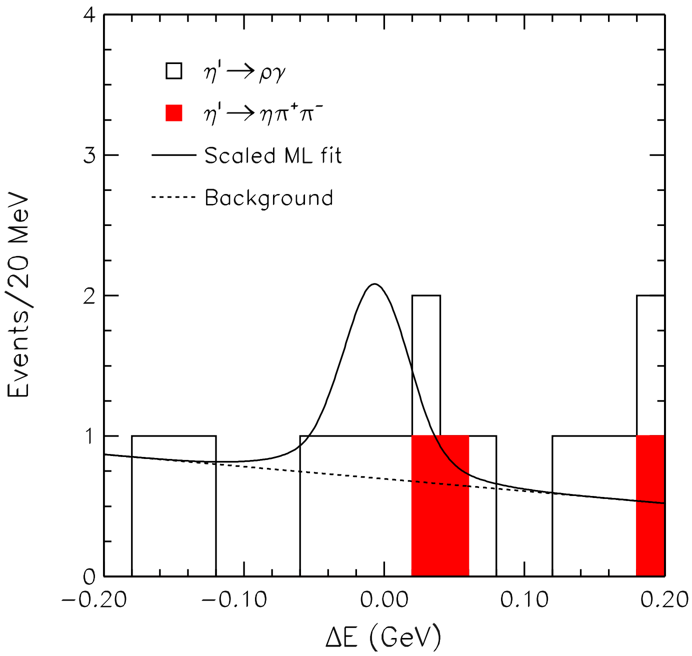

FIG. 7. Projection of ΔE for $B^0 \to \eta' K^0$.

REFERENCES

[1] J.P. Alexander and B.H. Behrens, Proceedings of the *Second International Conference on B Physics and CP Violation*, Honolulu, Hawaii, March 1997.

[2] J. Roy, Proceedings of the 1996 DPF Divisional Meeting, Minneapolis, MN, August, 1996.

[3] M. S. Alam *et al.*, CLEO CONF 97-23, contribution to this conference, August 1997.

[4] J.G. Smith, talk presented at the *1997 Aspen Winter Conference on Particle Physics*, Aspen, Colorado, January 1997.

[5] L.-L. Chau, *et al.*, Phys. Rev. D **43**, 2176 (1991).

[6] A. Deandrea, *et al.*, Phys. Lett. B **320**, 170 (1994).

[7] D. Du and L. Guo, Z. Phys. C **75**, 9 (1997).

[8] See for instance R. Fleischer, Int. J. Mod. Phys. **A12**, 2459 (1997) and Ref. [13].

[9] H.J. Lipkin, Phys. Lett. **B254**, 247 (1991).

[10] D. M. Asner *et al.*, CLEO CONF 97-13, contribution to this conference, August 1997.

[11] K. Berkelman, CLEO Internal Note, September 1996.

[12] F. Yuan and K-T. Chao, preprint hep-ph/9706294, June 1997 and references therein.

[13] A. Ali and C. Greub, preprint DESY 97-126 (hep-ph/9707251), July 1997.

[14] H-Y. Cheng and B. Tseng, preprint IP-ASTP-03-97, NTU-TH-97-08 (hep-ph/9707316), July 1997.

[15] I. Halperin and A. Zhitnitsky, preprint hep-ph/9704412, April 1997; I. Halperin and A. Zhitnitsky, hep-ph/9705251, May 1997; E.V. Shuryak and A. Zhitnitsky, hep-ph/9706316, June 1997.

[16] I. Dunietz, J. Incandela, F. Snider and H. Yamamoto, preprint FERMILAB-PUB-96/421-T (hep-ph/9612421), December 1996.
[17] A. Datta, X-G. He, and S. Pakvasa, preprint UH-511-864-97, ISU-HET-97-07 (hep-ph/9707259), July 1997.
[18] A. Kagan and A. Petrov, preprint UCHEP-27, UMHEP-443 (hep-ph/9707354), July 1997.
[19] M. Davier, Nuclear Physics B (Proc. Suppl.) **55C**, 395 (1997) (Proceedings of *TAU96: Fourth Workshop on Tau Lepton Physics*, Estes Park, Colorado, September 16-19, 1996, ed. J.G. Smith and W. Toki.)
[20] CLEO Collaboration, Y. Kubota *et al.*, Nucl. Instrum. Methods A **320**, 66 (1992).
[21] CLEO Collaboration, D.M. Asner *et al.*, Phys. Rev. D **53**, 1039 (1996).
[22] Particle Data Group, R.M. Barnett *et al.*, Phys. Rev. D **54**, 1 (1996).